University of Reading

The therapeutic potential of soluble activin type IIB receptor treatment in a limb girdle muscular dystrophy type 2D mouse model

Article

Accepted Version

Creative Commons: Attribution-Noncommercial-No Derivative Works 4.0

Alqallaf, A., Engelbeen, S., Palo, A., Cutrupi, F., Tanganyika-de Winter, C., Plomp, J., Vaiyapuri, S. ORCID: https://orcid.org/0000-0002-6006-6517, Aartsma-Rus, A., Patel, K. and Putten, M. v. (2022) The therapeutic potential of soluble activin type IIB receptor treatment in a limb girdle muscular dystrophy type 2D mouse model. Neuromuscular Disorders, 32 (5). pp. 419-435. ISSN 0960-8966 doi: 10.1016/j.nmd.2022.03.002 Available at https://centaur.reading.ac.uk/104798/

It is advisable to refer to the publisher's version if you intend to cite from the work. See Guidance on citing.

To link to this article DOI: http://dx.doi.org/10.1016/j.nmd.2022.03.002

Publisher: Elsevier

All outputs in CentAUR are protected by Intellectual Property Rights law, including copyright law. Copyright and IPR is retained by the creators or other copyright holders. Terms and conditions for use of this material are defined in the End User Agreement.

University of Reading

www.reading.ac.uk/centaur

CentAUR

Central Archive at the University of Reading

Reading's research outputs online

ARTICLE IN PRESS
JID: NMD [m5+;April 22, 2022;1:14]
Available online at www.sciencedirect.com
ScienceDirect
Neuromuscular Disorders xxx (xxxx) xxx
www.elsevier.com/locate/nmd

The therapeutic potential of soluble activin type IIB receptor treatment in a limb girdle muscular dystrophy type 2D mouse model

Ali Alqallaf[a,b,1], Sarah Engelbeen[c,1], Angela Palo[a], Federico Cutrupi[a], Christa Tanganyika-de Winter[c], Jaap Plomp[d], Sakthivel Vaiyapuri[e], Annemieke Aartsma-Rus[c], Ketan Patel[a,*], Maaike van Putten[c,**]

[a] *School of Biological Sciences, University of Reading, Reading, United Kingdom*
[b] *Medical Services Authority, Ministry of Defence, Kuwait*
[c] *Leiden University Medical Center, Department of Human Genetics, Leiden, the Netherlands*
[d] *Leiden University Medical Center, Department of Neurology, the Netherlands*
[e] *School of Pharmacy, University of Reading, Reading, United Kingdom*

Received 7 November 2021; received in revised form 13 February 2022; accepted 2 March 2022
Available online xxx

Abstract

Limb girdle muscular dystrophy type 2D (LGMD2D) is characterized by progressive weakening of muscles in the hip and shoulder girdles. It is caused by a mutation in the α-sarcoglycan gene and results in absence of α-sarcoglycan in the dystrophin-glycoprotein complex. The activin type IIB receptor is involved in the activin/myostatin pathway, with myostatin being a negative regulator of muscle growth. In this study, we investigated the effects of sequestering myostatin by a soluble activin type IIB receptor (sActRIIB) on muscle growth in *Sgca*-null mice, modelling LGMD2D. Treatment was initiated at 3 weeks of age, prior to the disease onset, or at 9 weeks of age when already in an advanced stage of the disease. We found that early sActRIIB treatment resulted in increased muscle size. However, this led to more rapid decline of muscle function than in saline-treated *Sgca*-null mice. Furthermore, no histopathological improvements were seen after sActRIIB treatment. When initiated at 9 weeks of age, sActRIIB treatment resulted in increased muscle mass too, but to a lesser extent. No effect of the treatment was observed on muscle function or histopathology. These data show that sActRIIB treatment as a stand-alone therapy does not improve muscle function or histopathology in *Sgca*-null mice.
© 2022 Elsevier B.V. All rights reserved.

Keywords: Myostatin; Muscle hypertrophy; Muscle growth; LGMDR3.

1. Introduction

Limb girdle muscular dystrophy (LGMD) is a large heterogeneous group of neuromuscular disorders characterized by slow progressive weakening of muscles of the hip and shoulder girdles. There are over 30 subtypes, which can be divided, based on their mode of inheritance, into autosomal dominant (LGMD1) and autosomal recessive (LGMD2) subgroups [1,2].

Sarcoglycanopathies are the most common forms of LGMD2 and are caused by mutations in one of the sarcoglycans (α-, β-, γ-, and δ-sarcoglycan). Sarcoglycans are essential components of the dystrophin-glycoprotein complex, which links the intracellular cytoskeleton with the extracellular matrix and provides muscle fibres with stability during contractions. Loss of one of the sarcoglycans results in impaired structural integrity and consequently contraction-induced muscle damage [2,3]. Mutations in α-sarcoglycan

* Corresponding author at: School of Biological Sciences, University of Reading, Reading UK RG6 6UB.
** Corresponding author at: Leiden University Medical centre, Department of Human Genetics, Leiden, the Netherlands.
E-mail addresses: ketan.patel@reading.ac.uk (K. Patel), m.van_putten@lumc.nl (M. van Putten).
[1] Equal author contribution.

https://doi.org/10.1016/j.nmd.2022.03.002
0960-8966/© 2022 Elsevier B.V. All rights reserved.

Please cite this article as: A. Alqallaf, S. Engelbeen, A. Palo et al., The therapeutic potential of soluble activin type IIB receptor treatment in a limb girdle muscular dystrophy type 2D mouse model, Neuromuscular Disorders, https://doi.org/10.1016/j.nmd.2022.03.002

are found in LGMD2D (LGMD R3 α-sarcoglycan-related), which is the most common form of sarcoglycanopathies [1]. LGMD2D is characterized by severe, progressive weakness of proximal muscles [1]. It has an early disease onset with patients becoming wheelchair-dependant around the age of 15 years [1,4]. Respiratory failure and cardiac complications occur in these sarcoglycanopathies [1,2]. There is no cure for sarcoglycanopathies at the moment.

Myostatin, mainly expressed by skeletal muscle, is a member of the TGF-beta family. It is a negative regulator of muscle growth and acts via the activin type IIB receptor (ActRIIB) [5,6]. Treatment with soluble ActRIIB (sActRIIB) can sequester myostatin and prevent it from binding to its endogenous receptor, thereby enhancing muscle growth [5,7]. We and others have shown that attenuating myostatin signalling results in a robust increase in muscle mass in rodents at any stage in their lifespan [8,9], although this is not accompanied by proportionate changes in force generation [9]. However, the clinical value of these studies has to be viewed in the light that the experimental model was one which displayed normal muscle growth. A number of studies have tested myostatin antagonists in models of muscle wasting [7,10], which are more clinically relevant.

It has been shown that treatment with sActRIIB can increase muscle mass and alleviate some of the disease symptoms in a mouse model of Duchenne muscular dystrophy (DMD) [7,11,12]. In addition to mouse experiments, sActRIIB treatment was well tolerated in a single-dose phase I trial. A study in healthy postmenopausal women and a phase II clinical trial in DMD boys showed increased lean mass [6,13]. However, in the mouse model of DMD, we have shown that the hypertrophic muscle induced by myostatin antagonists was functionally compromised and predisposed to fatigue and metabolic myopathy [14].

In this study, we investigated the effects of sActRIIB administration in the *Sgca*-null mouse model for LGMD2D, which is α-sarcoglycan deficient and recapitulates the human pathology well. Based on natural history studies, it is known that these mice develop muscle pathology and present with functional impairments from 4 weeks of age onwards [15,16]. We hypothesized that the attenuation of myostatin would prevent disease pathological and functional characteristics when administered to *Sgca*-null mice prior to disease onset, and that treatment started at advanced stages of the disease would result in relative improvements of muscle function and quality. While sActRIIB treatment increased muscle mass regardless of the timing of treatment initiation, there was no improvement of muscle function or histopathology observed in the *Sgca*-null mouse model for LGMD2D.

2. Material and methods

2.1. Mice and study setup

Sgca-null (B6.129S6-Sgca^{tm2Kcam}/J) and C57BL/6J mice were derived from in-house breeding couples. They were housed in individually ventilated cages (IVC) at 20.5^{0}C with 12 hour dark/light cycles, and had *ad libitum* excess to water and RM3 chow (SDS, Essex, United Kingdom) throughout the study duration. All animal experiments were approved by the Animal Experiment Committee of the Leiden University Medical centre.

Mice were randomly divided over experimental groups that consisted of $n=6$ males. *Sgca*-null mice received intraperitoneal injections of either 5 mg/kg sActRIIB in 100 µl saline, or saline alone, two times per week for a duration of six weeks. C57BL/6J males served as controls and were treated with saline only. Treatments started at either 3 weeks of age (prior to initiation of the disease pathology) or at 9 weeks of age (during the acute phase of the pathology).

To assess muscle functionality throughout the study, mice were weekly subjected to a non-invasive functional test regimen on consecutive days. One test was performed per day, and the order was kept constant throughout the study duration. The functional tests were considered sensitive and reliable, based on our natural history studies [15,16]. Tests were executed according to standardized operating procedures from the TREAT-NMD network for *mdx* mice wherever possible [17]. All mice successfully complied with the functional test regimen.

2.2. Functional test regimen

2.2.1. Two limb hanging test

The mouse was hovered over a metal wire which was secured above a cage filled with bedding. Once the mouse grasped the wire with its forelimbs, the experimenter released the mouse and started the timer. The mouse was allowed to use all four limbs and the tail during the hanging test if able to so. The hanging time until fall was recorded. If this was less than 600 s, mice got a maximum of two additional attempts to do so. Mice were directly retested after falling. The maximum hanging time was used for analysis.

2.2.2. Four limbs hanging test

In the four limbs hanging test, a mouse was placed on a grid after which the grid was inverted so that the mouse was hanging above a cage filled with bedding. Mice were given three attempts to hang for 600 s, and were directly retested when they fell off earlier. The maximum hanging time until fall was recorded.

2.2.3. Forelimb gripstrength

The forelimb gripstrength of mice was measured using a grid attached to an isometric force transducer (Columbus Instruments, USA). Hereto, the mouse was handled by its tail and hovered above the grid until it grasped the grid with both forelimbs. When pulled away from the grid, the maximal force applied to the grid by the mouse was recorded. This was repeated three times in a row after which the mouse had a short resting period of 1 min. Thereafter, four additional sets of three pulls, each followed by a resting period, were executed so that each mouse pulled 15 times in total. The

three highest values obtained were averaged and normalized to body weight.

2.3. Respiratory function analysis

Respiration rate and depth of mice were non-invasively measured with whole-body plethysmography (RM-80; Columbus Instruments, Columbus, OH, USA) on a weekly basis. After an acclimatization period of 30 s, the respiration signal was recorded for two minutes. A Minidigi digitizer and the Axoscope 10 software were used to digitize the signal (Axon Instruments/Molecular Devices, Sunnyvale, CA, USA), which was analysed off-line with the event detection feature of the Clampfit 10 program (Axon Instruments/Molecular Devices). The respiration rate and amplitude was analysed, the latter was normalized for body weight.

2.4. Creatine kinase level measurement

For all cohorts, creatine kinase (CK) levels were measured at baseline, three and five weeks after treatment initiation, and prior to sacrifice. Hereto, blood was taken via a small cut in the tail vein and collected in heparin-coated microvette tubes (Sarstedt, Numbrecht, Germany). Samples were kept on ice and plasma was obtained after centrifugation at 13,000 rpm for 5 min at 4 °C. Plasma CK levels were measured on the Reflotron Sprint system with CK Reflotron strips (Roche, Diagnostics, Basel, Switzerland).

2.5. In situ muscle physiology of the tibialis anterior

Two weeks after the final injection, function of the right tibialis anterior muscle was assessed. Mice were anaesthetized with 2% isoflurane and placed on a thermopad to maintain the body temperature at 37 °C during the whole procedure. After anesthetization, the tendon of the tibialis anterior was dissected from the surrounding tissue and a thread was secured around it and tied into a loop. The sciatic nerve was exposed and all branches were cut away except for the common peroneal nerve, which stimulates the tibialis anterior. The mouse was placed on a rig with the foot tightly secured with tape and the knee immobilized using a needle to avoid unwanted movement of the leg. The tendon of the tibialis anterior was then attached to the lever arm of the force transducer via a custom made S-hook. The tibialis anterior was stimulated via the distal part of the peroneal nerve with bipolar platinum electrodes. Data was acquired with a Lab-view-based dynamic muscle data acquisition and analysis system (Aurora Scientific, Aurora, Ontario, Canada).

Mice underwent a warming-up protocol of five stimulations of 50 Hz spaced one min apart and optimal muscle length (L_O) was determined by a series of twitches at increasing resting tension. Thereafter, the maximum isometric tetanic force (P_O) was determined from the plateau of the force-frequency relationship after a series of stimulations at 10, 30, 40, 50, 80, 100, 120, 150 and 180 Hz which were spaced one min apart. The specific force (N/cm^2) was determined by dividing P_O by the cross-sectional area using the following formula: muscle weight (g)/ [tibialis anterior fibre length (cm) x 1.06 (g/cm^3)]. The tibialis anterior muscle's susceptibility to contraction-induced injury was measured after a resting period of five mins. Hereto, the muscle was stimulated at 120 Hz for 500 ms before lengthening at 10% of L_O at a velocity of 0.5 L_O/s. Once the stimulation ended, the muscle was returned to L_O at a rate of -0.5 L_O s^{-1}. The stimulation-stretch cycle was repeated every two mins for a total of 10 cycles. The maximum isometric force of the first contraction was used as the 100% baseline. Mice were euthanized by cervical dislocation after the procedure and muscles and tissues were isolated and weighed. Muscles were snap-frozen in isopentane and stored at −80 °C.

2.6. Muscle histology

Muscle tissues were mounted in OCT LT Embedding Compound (TAAB Laboratories Equipment Ltd, Aldermaston, United Kingdom), and snap-frozen in liquid nitrogen-cooled isopentane. Subsequently, the muscles were cryo-sectioned at a thickness of 15 μm using a cryostat (Bright Instruments OTF5000). Cryosections were collected on slides and stored at −80 °C for future histological analyses.

2.7. Immunohistochemistry (IHC)

Myosin heavy chain (MyHC) typing was analysed in the extensor digitorum longus (EDL) and soleus for all cohorts and additionally in the tibialis anterior for mice where treatment was initiated at 9 weeks of age. Dystrophin was visualized in the tibialis anterior for both cohorts. The muscle sections were incubated at room temperature for 15 min, and then a PAP pen (Agar scientific L4197S) was used to create a hydrophobic barrier to select the desired sections after which they were left to dry for 15 min. The slides were then washed 3 times in PBS for 5 min each, and subsequently incubated in permeabilisation buffer for 15 min. The sections were washed in PBS again before they were incubated in blocking wash buffer for 30 min, and incubated with the desired primary antibody (Supplementary Table. 1) overnight at 4 °C. The unbound primary antibodies were washed 3 times in blocking washing buffer 10 min each at room temperature. Simultaneously, the complementing secondary antibody (Supplementary Table. 2) was diluted in blocking wash buffer and incubated in the dark for 30 min. The secondary antibodies were applied to the slides and left for 1 h at room temperature. Excess antibodies were washed three times with blocking washing buffer 10 min each. At this stage, another primary antibody was added if a double stain was planned and the previous subsequent steps were repeated. Eventually, the sections were mounted with a drop of DAPI (1:2000 (Fisher Scientific D1306) with Dako fluorescence mounting medium (Dako North America Inc. REF S3023)). The slides were imaged using a Zeiss AxioImager epifluorescence microscope that was operated by

AxioVision SE64 Rel. 4.9.1 software. The exported images were stitched using Adobe Photoshop elements 2018 (Adobe, San Jose, CA, USA) software. Dystrophin max intensity, MyHC fibre type and muscle fibre area were quantified using ImageJ (National Institutes of Health, Bethesda, MD, USA) software. Dystrophin maximum intensity was analysed for the whole muscle section of the tibialis anterior. When quantifying the MyHC fibre types and fibre area, whole muscle sections were analysed for EDL and soleus, while for the tibialis anterior two fixed size boxes were analysed from the deep and superficial regions of the muscle.

2.8. Picro Sirius Red stain

Collagen levels were measured on Picro Sirius Red stained slides of tibialis anterior sections. The muscle sections were warmed at room temperature for 15 min, immersed in Bouin solution for 15 min in a 56 °C water bath, rinsed and washed in tap water for 15 min at room temperature. Then, they were stained with Picro Sirius Red (Abcam kit ab150681) for 1 hour. The slides were then quickly rinsed in two changes of acidified water (1000 ml of distilled water, 5 ml of glacial acetic acid) two dips each time. Furthermore, the sections were dehydrated in ethanol 100% three times, 5 min each. Xylene was used to clear the slides for 5 min, which was followed by mounting of the sections with DPX mounting media (Fisher, REF D/5319/05). The sections were imaged using a Zeiss AxioSkop bright field microscope that was operated by AxioVision SE64 Rel. 4.9.1 software. The exported images were stitched, and background noise was removed using Adobe Photoshop elements 2018 (Adobe, San Jose, CA, USA). A threshold analysis of the green channel was conducted on ImageJ (National Institutes of Health, Bethesda, MD, USA) software to quantify the percentage of fibrosis. The threshold was corrected for stained calcification.

2.9. Haematoxylin and eosin (H&E) staining

To quantify centrally nucleated fibres and unhealthy tissue in the tibialis anterior, EDL and soleus, muscle sections were stained with haematoxylin and eosin. Hereto, sections were retrieved from the −80 °C freezer, left to dry at room temperature for 15 min, and washed in phosphate buffer saline (PBS, Oxoid BR0014G) for 2 min. Harris haematoxylin (Sigma-Aldrich HHS16) was used in a regressive staining for 1.5 mins. The differentiation step was achieved by immersing the slides twice in 70% acidic alcohol (200 ml 70% ethanol (Sigma-Aldrich 32,221–2.5L-M) + 200 µl 37% HCl (Fisher Scientific 7647–01–0)), followed by washing the slides under running tap water for 5 min. Eosin 1% (160 ml 70% ethanol + 40 ml Eosin Y (Sigma-Aldrich 318,906–500ML), 5 wt% solution in water = 200 ml of 1% Eosin)) was used as a counterstain by leaving the slides in it for 2 min. Subsequently, a dehydration series was performed in ethanol at increasing concentrations. To displace the ethanol, the sections were washed in xylene (Fisher Scientific 10,588,070) for 3 mins each. DPX mounting media (Fisher, REF D/5319/05) was applied to mount the sections. The sections were imaged using a Zeiss AxioSkop bright field microscope that was operated by the AxioVision SE64 Rel. 4.9.1 software. The exported images were stitched, and background staining was removed using Adobe Photoshop elements 2018 (Adobe, San Jose, CA, USA). The ImageJ software (National Institutes of Health, Bethesda, MD, USA) was used to quantify the percentage of centrally nucleated (CN) fibres in whole muscle sections for the EDL and the soleus, and two fixed size areas were analysed for both deep and superficial regions of the TA muscle. The colour deconvolution plugin (https://imagej.net/Deconvolution) was applied to quantify the area of unhealthy tissue (necrotic, fibrotic and recently regenerated tissue).

2.10. Succinate dehydrogenase (SDH)

The metabolic status of muscle fibres was assessed in the EDL and soleus with succinate dehydrogenase (SDH) staining. The muscle sections were retrieved from the −80 °C freezer and left to dry at room temperature for 15 mins. A PAP pen (Agar scientific L4197S) was used to create a hydrophobic barrier to select the desired sections and left to dry for 15 min. The succinate and nitro blue tetrazolium (NBT) stock solutions were placed on ice to prepare the final reaction solution. The sections were rehydrated with PBS for 5 mins before adding the reaction solution comprised of NBT (2 ml), succinate solution (0.2 ml) and one crystal of phenazine methosulfate. The sections were stained with the final mixture for 1 – 2 min until a magenta colour solution was observed. The reaction was stopped by washing the sections with distilled water for 1 min. Subsequently, the sections were fixed with formal calcium, and mounted with DPX mounting media (Fisher, REF D/5319/05). The sections were imaged using a Zeiss AxioSkop bright field microscope that was operated by the AxioVision SE64 Rel. 4.9.1 software. The exported images were stitched with Adobe Photoshop elements 2018 (Adobe, San Jose, CA, USA). The ImageJ software was utilised to quantify the ratio of dark and lightly stained fibres in whole muscle sections of the EDL and soleus.

2.11. RNA isolation and qPCR

Tissues were homogenized with a MagNALyser (Roche Diagnostics) in zirconium bead pre-filled tubes (OPS Diagnostics, Lebanon, USA) in the presence of TriSure reagent (Bioline, London, UK). Total RNA was isolated using the TriSure reagent method according to the manufacturer's instructions. Afterwards, samples were further cleaned up with a NucleoSpin RNA kit (Macherey-Nagel, Düren, Germany), according to the manufacturer's instruction. Complementary DNA (cDNA) was made from 1 µg of RNA in the presence of random hexamers, dNTPs, Tetro reverse transcriptase and 5x reaction buffer (Bioline). Expression levels were assessed with a quantitative PCR (qPCR) for genes involved in regeneration (myosin heavy chain 3 (*Myh3*), paired box 7 (*Pax7*), myogenin (*MyoG*), NAPDH

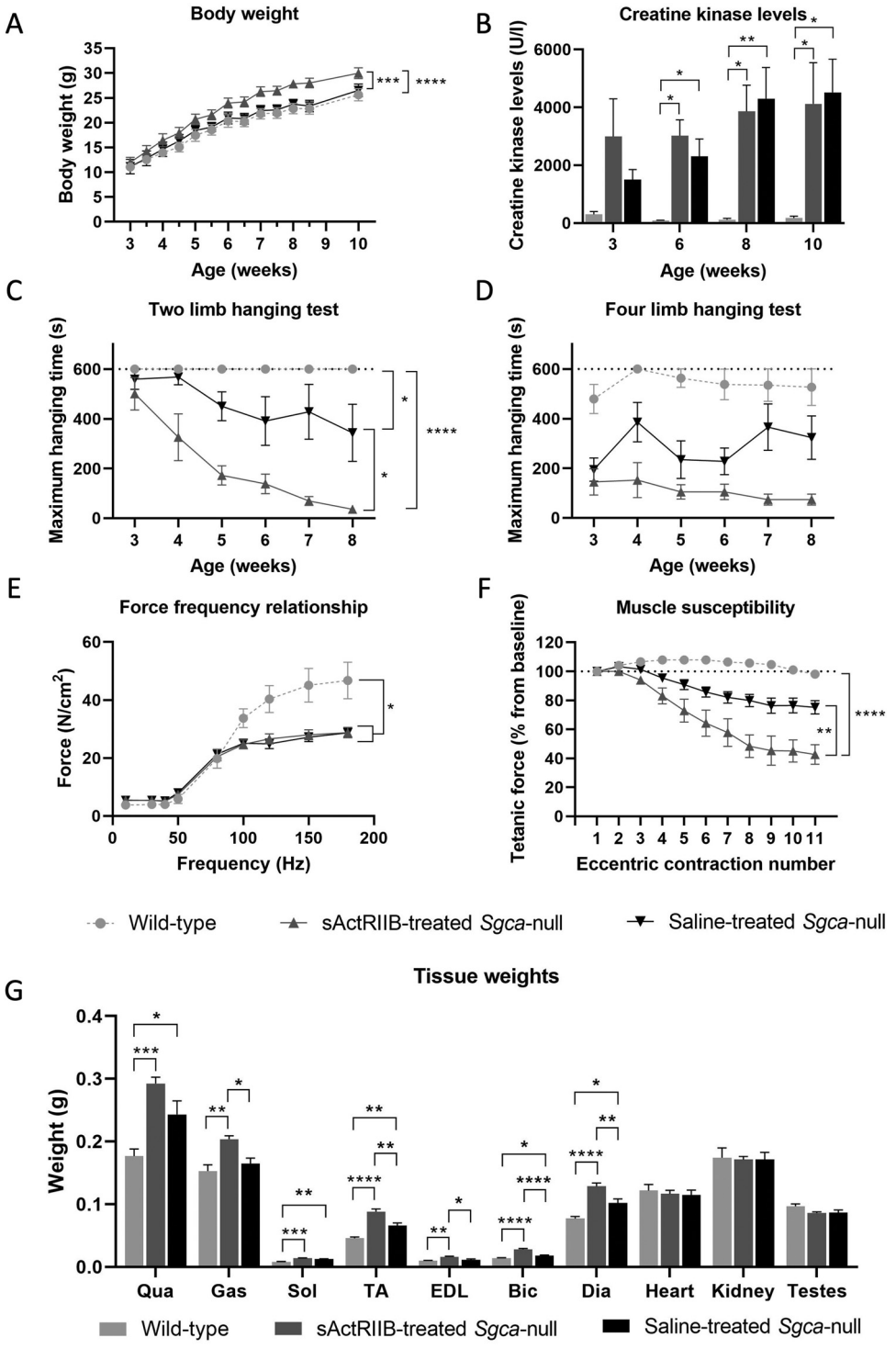

Fig. 1. Effect of sActRIIB-treatment initiated at 3 weeks of age on body weight, creatine kinase levels and muscle function. (A) Bodyweight. (B) Creatine kinase levels. (C) Two limb hanging test. (D) Four limb hanging test. (E) Force frequency relationship of the tibialis anterior. (F) Susceptibility of the tibialis anterior to damage during eccentric contractions. (G) Muscle and tissue weights. $^{*}P<0.05$, $^{**}P<0.01$, $^{***}P<0.001$, $^{****}P<0.0001$. $N=6$ per group.

oxidase 2 (*Nox2*), inflammation (cluster of differentiation 68 (*Cd68*), lectin galactosidase binding soluble 3 (*Lgals3*)) and adipogenesis (peroxisome proliferator-activated receptor γ (*PPAR*γ)). qPCRs were performed in triplicates per sample with forward and reverse primers (Supplementary Table 3) and ready to use SensiMix (Bioline) in a LightCycler 480 (Roche). Expression levels were analysed with the LinReg qPCR software and levels were normalized to the expression levels of the housekeeping gene *Hmbs* (tibialis anterior and soleus), *Hprt* (gastrocnemius) and *Gapdh* (EDL). Even though 17 housekeeping genes were tested (*Hmbs, Gapdh, Pak1ip1, Srp14, Zfp91, Ap3d1, Hprt, Htatsf1, Rpl13a, Sdha, Actb,*

Cdc40, Fbxw2, Mon2, B2m, Csnk2a2, Hpsf), none of them was suitable for the EDL of mice in which treatment was initiated at 3 weeks of age.

2.12. Statistical analyses

Data analyses were performed with either GraphPad Prism (GraphPad Software, San Diego, California USA, version 8.1.1) or SPSS (IBM SPSS Statistics for Windows, Version 25.0. Armonk, NY: IBM Corp.). Values are presented as means ± SEM. $P<0.05$ was considered statistically significant for all tests performed.

Body weight, hanging tests, gripstrength and respiratory assessment data was analysed with a linear mixed-effects model using fixed effects for treatment and time interaction and random effects for time. Creatine kinase levels were analysed with a two-way ANOVA for followed by a Bonferroni's multiple comparison test for each timepoint. Area under curve (AUC) values were calculated per mouse per treatment group for the force frequency relationship and the initial force drop over number of contractions per treatment group and compared between groups with a one-way ANOVA followed by a Bonferroni's multiple comparison test. Differences in muscle and tissue weights were analysed with a one-way ANOVA followed by a Bonferroni's multiple comparison test to compare between the different groups. Histological data was analysed with a one-way ANOVA and Bonferroni's multiple comparison test to determine differences between groups. Differences in gene expression were analysed as well with a one-way ANOVA followed by the Bonferroni's multiple comparison test.

3. Results

3.1. sActRIIB treatment increases muscle mass, but does not prevent deterioration of muscle function in young Sgca-null mice

To study whether sActRIIB treatment was capable of preventing functional impairment and muscle pathology, *Sgca*-null mice were injected with sActRIIB two times per week for six weeks starting at 3 weeks of age (prior to the development of any pathological features). Mice were weighed two times per week and muscle function was assessed with a series of functional tests. Between the age of 3 and 10 weeks, we observed a steady increase in body weight in all cohorts (Fig. 1A). As expected, sActRIIB treatment resulted in an increased body weight over time compared to saline treated *Sgca*-null and wild-type mice. Creatine kinase (CK) levels were elevated in *Sgca*-null compared to the wild-type mice reaching statistical significance at 3, 6 and 10 weeks of age. sActRIIB-treated *Sgca*-null mice had statistically significantly increased CK levels at 6 and 8 weeks of age, as compared to wild-type mice (Fig. 1B). CK levels did not differ between the two *Sgca*-null cohorts.

Muscle function and fatigability were assessed with the two and four limb hanging tests. In the forelimb hanging test, sActRIIB-treated *Sgca*-null mice showed a significant decline over time compared to saline-treated *Sgca*-null mice and wild-type mice. Saline-treated *Sgca*-null mice performed significantly worse than wild-type mice over time (Fig 1C). While both *Sgca*-null groups performed significantly worse from the start of the experiment compared to wild-type mice in the four limb hanging test (intercept of $P<0.0001$ for both *Sgca*-null groups compared to wild-type), it did not significantly deteriorate with age (Fig. 1D). Muscle strength was assessed with the forelimb gripstrength which was similar for all groups (Supplementary Fig. 1A). Since the diaphragm is most severely affected in dystrophic mouse models, we assessed respiratory function with the whole-body plethysmography. No changes were observed in respiration amplitude and respiration rate between the groups (Supplementary Fig. 1C-E).

Two weeks after the last injection, physiology of the tibialis anterior was investigated . During the force-frequency protocol, wild-type muscles produced significantly greater forces than *Sgca*-null muscles. Treatment with sActRIIB did not affect the observed muscle weakness (Fig. 1E). No differences were observed for absolute force between groups (Supplementary Fig. 1B). Following a series of eccentric contractions, we saw a decrease in tetanic force of ∼24.8% ± 4.6% in saline-treated *Sgca*-null mice compared to wild-type. An even more pronounced, and statistically significant, force deficit was observed in the sActRIIB-treated *Sgca*-null mice (57.3% ± 6.8%) compared to saline-treated *Sgca*-null and wild-type mice (Fig. 1F).

After the muscle physiology assessment, mice were euthanized and muscles and tissues were isolated and weighed. Saline-treated *Sgca*-null mice had a significantly heavier quadriceps, soleus, tibialis anterior, biceps and diaphragm compared to wild-types. sActRIIB treatment further increased weight of the gastrocnemius, tibialis anterior, EDL, biceps and the diaphragm compared to saline-treated *Sgca*-null mice. All examined skeletal muscles had a statistically significantly increased weight in the sActRIIB-treated *Sgca*-null mice, compared to wild-types (Fig. 1G). No differences were seen in the heart, kidney and testes weights.

3.2. Attenuation of myostatin signalling initiated in young Sgca-null mice does not resolve disease histopathological features in skeletal muscle

To determine the cause of the increased muscle mass in *Sgca*-null mice compared to wild-type, but more particularly the increase in muscle mass following sActRIIB treatment, we examined muscle sections of the EDL (a fast-twitch muscle) and the soleus (a slow-twitch muscle), using a panel of MyHC specific antibodies followed by morphometric analysis for fibre size (Fig. 2A).

First, we profiled the composition of the EDL, which showed a statistically significant change only in the type IIB fibres of saline-treated *Sgca*-null mice compared to wild-type mice. In contrast, there was a change in the proportion of

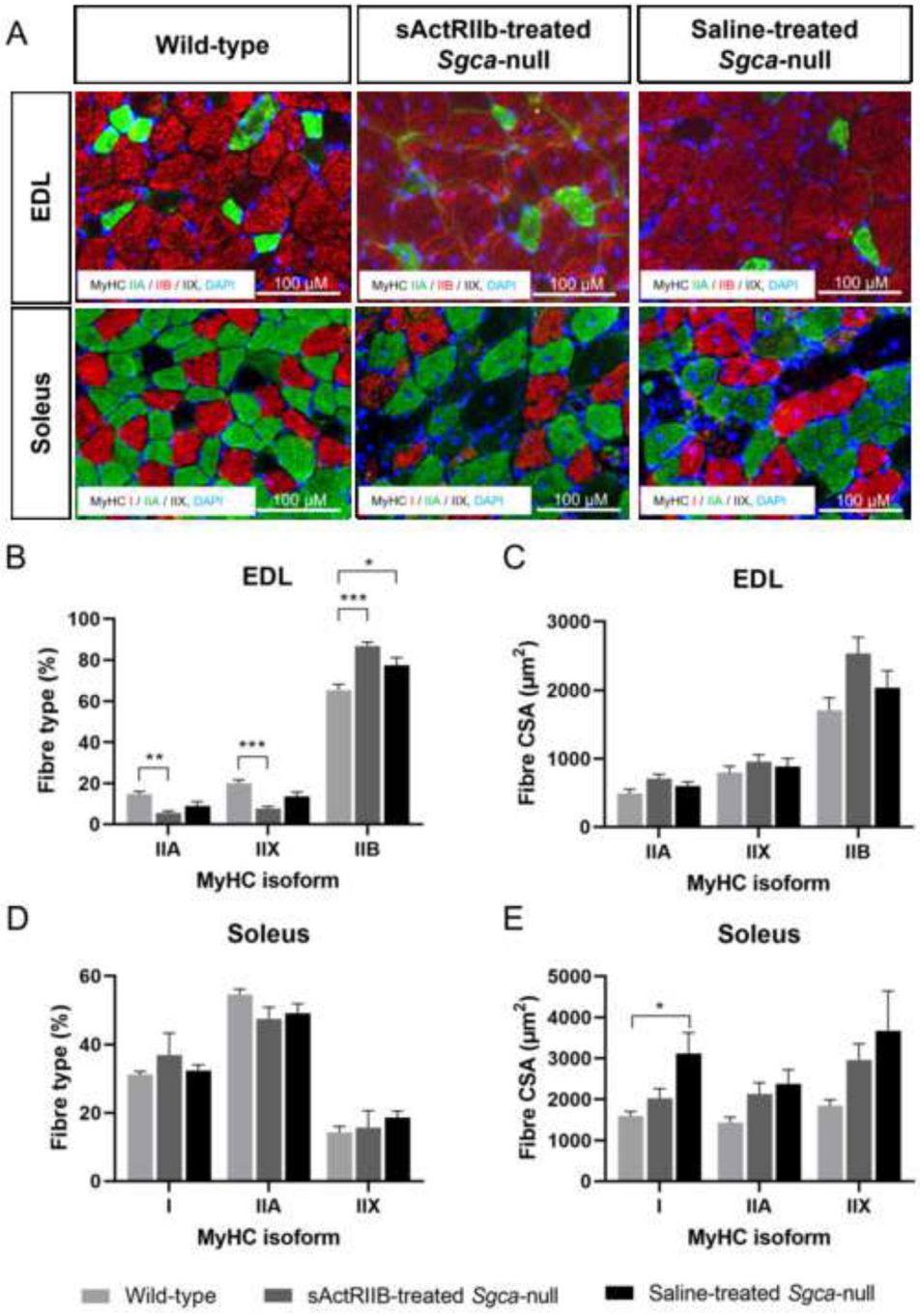

Fig. 2. Effect of sActRIIB-treatment initiated at 3 weeks of age on MyHC fibre type characteristics. (A) Representative images of EDL and soleus muscles from wild-type, sActRIIB-treated *Sgca*-null, and saline-treated *Sgca*-null mice; EDL: green= MyHC IIA, red= MyHC IIB, blue/DAPI = nuclei, soleus: green= MyHC IIA, red= MyHC Type I, blue/DAPI = nuclei. (B) Percentage of MyHC fibre types IIA, IIX, and IIB in EDL. (C) Average fibre CSA of non-centrally nucleated MyHC isoforms in EDL. (D) Percentage of MyHC fibre types I, IIA, and IIX in soleus. (E) Average fibre CSA of non-centrally nucleated MyHC isoforms in soleus. $^{*}P<0.05$, $^{**}P<0.01$, $^{***}P<0.001$, $^{****}P<0.0001$. B-E: $N=5$ per group.

all fibre types when comparing sActRIIB-treated *Sgca*-null to wild-type mice. In particular, there was a decrease in proportion of type IIA and IIX, whereas the proportion of type IIB fibres had increased (Fig. 2B). Next, we examined fibre size for these specific forms of MyHC. No statistically significant differences were seen in fibre size of the different MyHC isoforms between the different groups (Fig. 2C). We analysed the cross-sectional area data in detail to determine whether the fibre hypertrophy phenotype seen in the EDL of *Sgca*-null mice was global or resulted from specific fibres by plotting a frequency distribution graph against cross-sectional area. We found a general shift towards larger fibres for all fibre types (Supplementary Fig. 2A-C). Examination of the soleus showed that its composition was unaffected by either genotype or intervention (Fig. 2D). Additionally, through fibre size analysis we observed that saline-treated *Sgca*-null mice

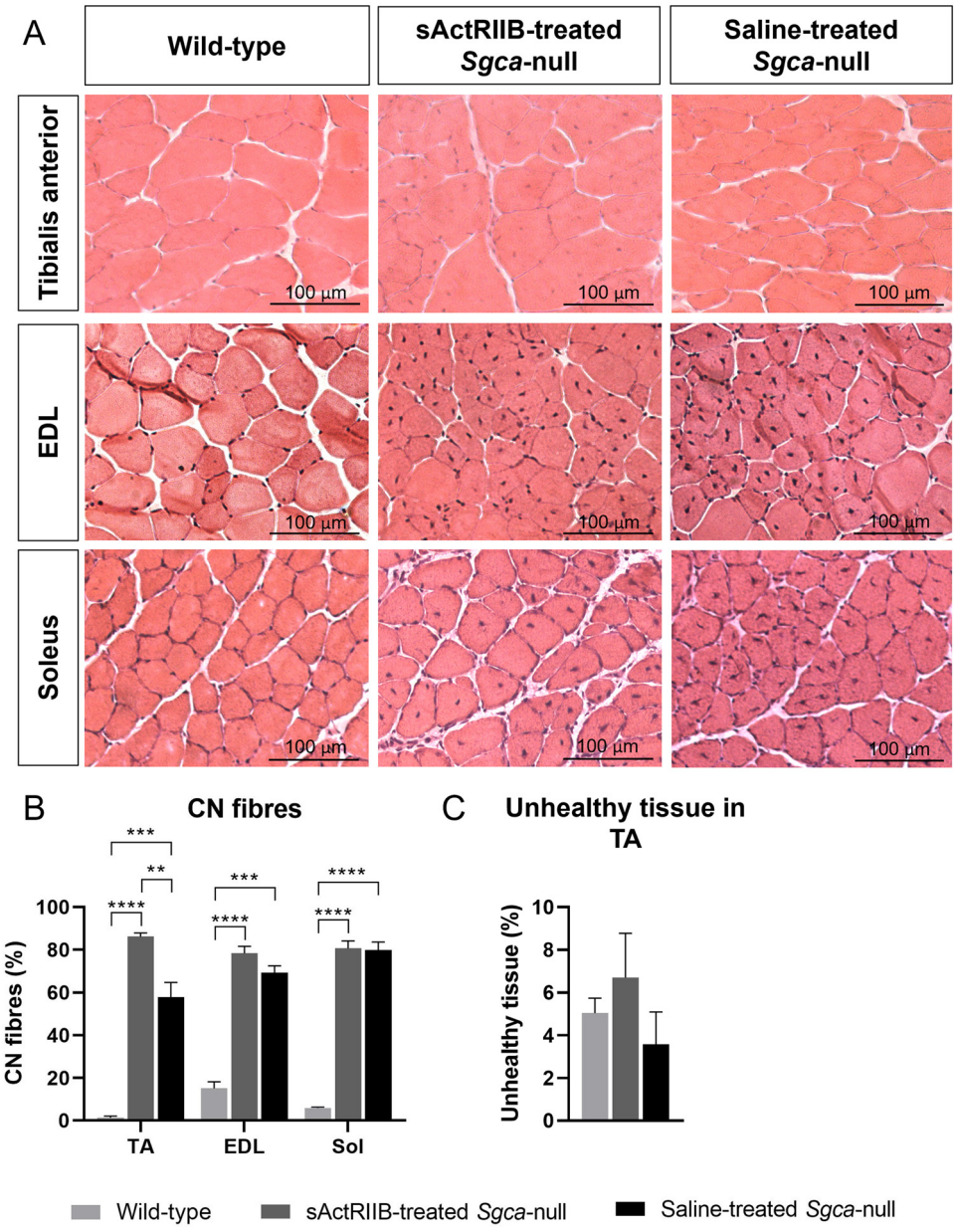

Fig. 3. Skeletal muscle histopathology of sActRIIB-treatment in mice initiated at 3 weeks of age. (A) Representative images of H&E stained cross-sections of tibialis anterior (TA), EDL and soleus. (B) Quantification of the percentage of CN fibres in muscle sections. (C) Quantification of percentage of unhealthy tissue in TA muscle; $N=5$ per group for EDL and soleus (Sol), $N=3$ per group for TA. ** $P<0.01$, *** $P<0.001$, **** $P<0.0001$.

had increased fibre size for all MyHC isoforms but reaching statistical significance only in type I fibres. Increases in fibre size for the MyHC isoforms were less pronounced in sActRIIB-treated mice (Fig 2E).

Next, we examined whether non-myocyte tissue contributed to muscle weight changes in the *Sgca*-null cohorts. To that end, we quantified the degree of fibrosis, the amount of unhealthy tissue and dystrophin expression in the tibialis anterior. We observed similar levels of fibrosis based on Picro Sirius Red staining in all three cohorts (Supplementary Fig. 3A-B). Lastly, we examined fibre integrity by quantifying the expression of dystrophin protein at the sarcolemma. The investigations failed to detect any difference in the amount of dystrophin between the three cohorts (Supplementary Fig. 3A,C).

Central nucleation is one of the hallmarks of histopathology in the *Sgca*-null model. We quantified the proportion of centrally nucleated fibres, and how this parameter was influenced by treatment. Indeed, we found central nucleation in the majority of fibres in the tibialis anterior, EDL and soleus of solely *Sgca*-null mice (Fig. 3A,B). Treatment with sActRIIB further increased the proportion of centrally nucleated fibres only in the tibialis anterior (Fig. 3B). No statistically significant differences were observed after the quantification of unhealthy tissue after H&E staining though a slight increase was observed for

the sActRIIB-treated *Sgca*-null mice compared to the other cohorts (Fig. 3A,C).

We also examined the impact of genotype and treatment on the metabolic status of muscle fibres by profiling the proportion of fibres displaying SDH activity (Supplementary Fig. 4A). Our analysis revealed no impact of either genotype or treatment in the proportion of dark SDH fibre in the EDL and soleus (Supplementary Fig. 4B-C). In summary, treatment of young *Sgca*-null mice with sActRIIB results in global muscle fibre hypertrophy without any change in non-muscle components. However, the increase in muscle mass is accompanied by force generation deficits and an increased susceptibility to fatigue.

3.3. sActRIIB treatment does not affect gene expression in young Sgca*-null mice*

Muscular dystrophies are characterized by continuous cycles of degeneration and regeneration. We, therefore, assessed regeneration with several markers (*Myh3, Pax7, MyoG* and *Nox2*) in the tibialis anterior, soleus and gastrocnemius. *Myh3*, expressed in newly formed regenerating myofibres, was increased in all *Sgca*-null mice compared to wild-type. This reached statistical significance in the tibialis anterior and gastrocnemius of saline-treated *Sgca*-null mice, and in the soleus and gastrocnemius of sActRIIB-treated *Sgca*-null mice (Fig. 4A). *Pax7,* involved in muscle stem cell proliferation, was not significantly different between the groups (Fig. 4B). *MyoG*, a marker expressed early in skeletal muscle differentiation, was only statistically significantly increased in the tibialis anterior of the *Sgca*-null groups (Fig. 4C). *Nox2,* involved in inflammation and regeneration, was increased in all *Sgca*-null samples, reaching statistical significance in the tibialis anterior and gastrocnemius. In the gastrocnemius, levels of sActRIIB-treated *Sgca*-null mice exceeded those of saline-treated *Sgca*-null mice (Fig. 4D).

Inflammation was assessed through expression levels of *Cd68* and *Lgals3*. Levels of both genes were statistically significantly increased in the tibialis anterior and gastrocnemius of *Sgca*-null mice (Fig. 4E-F). sActRIIB treatment further increased expression of *Cd68* and *Lgals3* in the gastrocnemius.

Adipogenesis was assessed by expression of *Pparγ* which has previously been shown to be a good marker for fat infiltration (doi: 10.1371/journal.pone.0182704). *Sgca*-null mice had lower levels of *Pparγ* than wild-types, reaching statistical significance in the tibialis anterior and soleus of saline-treated mice, and in the soleus of sActRIIB-treated animals (Fig. 4G).

3.4. sActRIIB treatment does not ameliorate disease pathology when initiated during the acute disease phase

To investigate whether sActRIIB treatment can ameliorate disease pathology in older mice, that already have extensive muscle pathology, treatment was initiated in *Sgca*-null mice aged 9 weeks. We subjected mice to the same assessments as the 3 weeks aged groups.

Saline- and sActRIIB-treated *Sgca*-null mice had a statistically significant increase in body weight over time compared to wild-type mice. While sActRIIB-treated *Sgca*-null mice were heavier than saline-treated mice over the course of the experiment, these differences were not statistically significant (Fig. 5A). Creatine kinase levels were elevated in *Sgca-null* mice compared to wild-type mice, reaching statistical significance in saline-treated *Sgca*-null mice at 9, 14 and 16 weeks of age (Fig. 5B). Both *Sgca*-null cohorts performed worse in the hanging tests compared to wild-type mice. While the intercept of the performance of *Sgca*-null mice was significantly different than in wild-type, saline-treated *Sgca*-null mice had a significantly different pattern in performance over time compared to sActRIIB-treated *Sgca*-null mice and wild-type mice (Fig. 5C). In the four limb hanging test, *Sgca*-null mice once again had a significant different intercept than wild-type mice but here the saline-treated *Sgca*-null mice only showed a significantly different pattern in performance over time compared to wild-type (Fig. 5D). In the forelimb gripstrength test, both *Sgca*-null groups had a significant different intercept and performance over time compared to wild-types (Supplementary Fig. 5A). Respiration rate for *Sgca*-null mice was significantly different from wild-type for both the intercept and the performance over time (Supplementary Fig. 5C). Respiration amplitude and normalized respiration amplitude was similar between all groups (Supplementary Fig. 5D-E).

Physiological assessments of the tibialis anterior were performed at 16 weeks of age, two weeks after the last injection. *Sgca*-null mice exhibited statistically significantly lower specific forces, compared to wild-type mice, in the force-frequency relationship analysis (Fig. 5E). There was no difference in specific force between the *Sgca*-null cohorts. Absolute force was comparable between all groups (Supplementary Fig. 5B). The resistance to lengthening contractions was equally impaired in both *Sgca*-null cohorts compared to wild-type mice (Fig. 5F).

Saline-treated *Sgca*-null mice had an increased weight of the quadriceps, soleus, tibialis anterior, biceps and diaphragm compared to wild-types. The increase in bodyweight after sActRIIB treatment was accompanied by an increased weight of the quadriceps, soleus, tibialis anterior, EDL, biceps and diaphragm compared to wild-type. Further gains in muscle weight were observed, compared to saline-treated *Sgca*-null mice, in the tibialis anterior and biceps. No differences were found in tissue weight for heart, kidney and testes (Fig. 5G).

3.5. Attenuation of myostatin signalling via sActRIIB in Sgca*-null mice during the acute phase does not mitigate disease histology in skeletal muscle*

Analysis of fibre composition for the EDL revealed a genotype-based shift towards faster-contracting fibres; a statistically significant decrease was observed in the

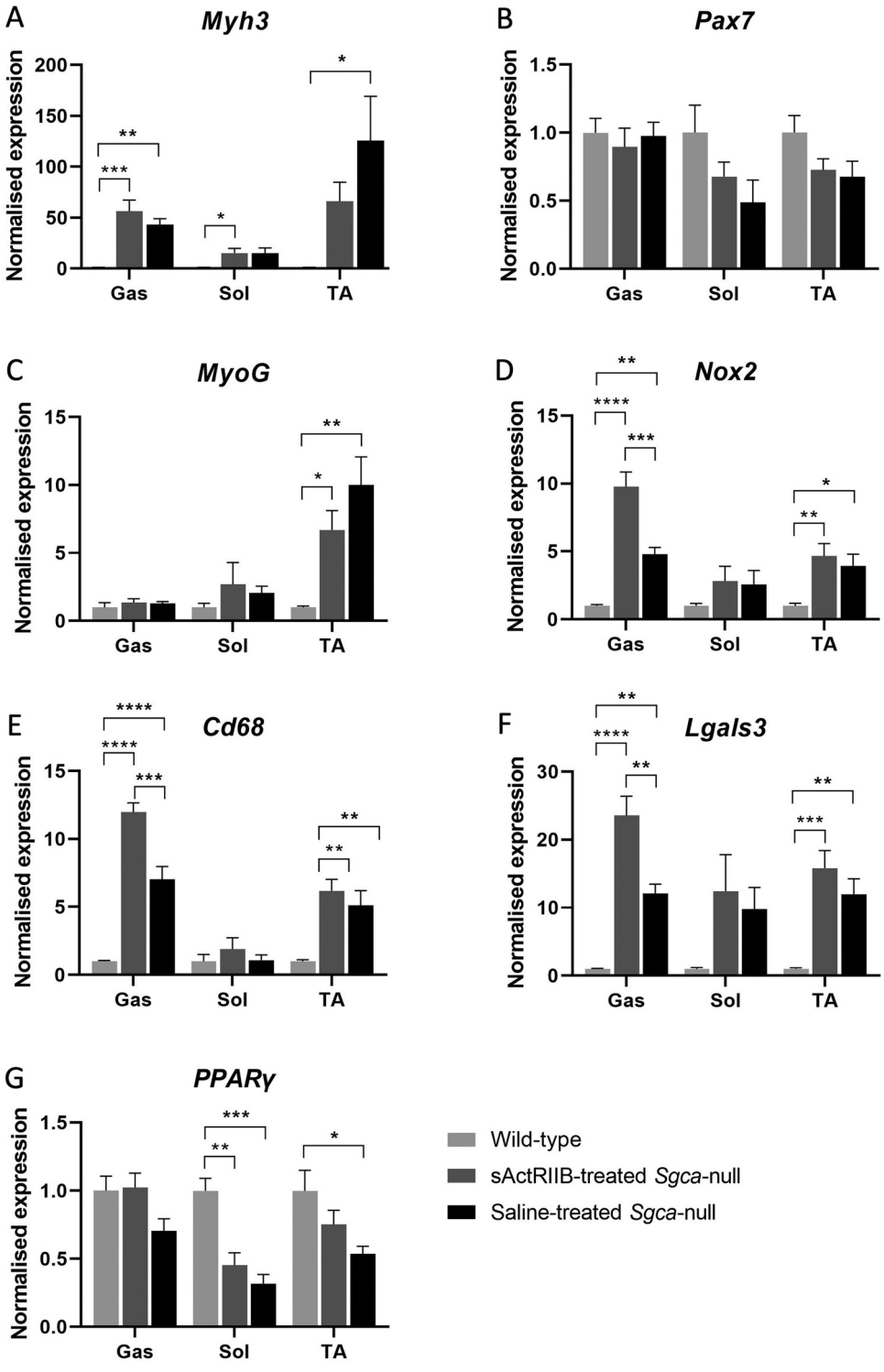

Fig. 4. Gene expression analyses of regeneration, inflammation and fatty infiltration markers of mice in which treatment started at 3 weeks of age. (A-D) Regeneration markers *Myh3*, *Pax7, MyoG* and *Nox2,* (E-F) inflammation markers *Cd68* and *Lgals3* and (G) fatty infiltration marker *Pparγ* in gastrocnemius (Gas), soleus (Sol) and tibialis anterior (TA). Expression levels were normalized for the housekeeping gene *Hmbs* (TA and Sol) and *Hprt* (Gas). $N=6$ per group. $^{*}P<0.05$, ** $P<0.01$, $^{***}P<0.001$, $^{****}P<0.0001$.

proportion of type IIA fibres, while type IIB fibres were more abundant in *Sgca*-null mice compared to wild-type mice (Fig. 6A-B). Characterisation of MyHC isoform-specific changes in cross-sectional area revealed only a trend for hypertrophy in type IIB fibres from sActRIIB-treated *Sgca*-null mice, compared to the other two cohorts (Fig. 6C). In contrast, sActRIIB-treated *Sgca*-null mice had a statistically significant decrease in the percentage of IIA fibres in

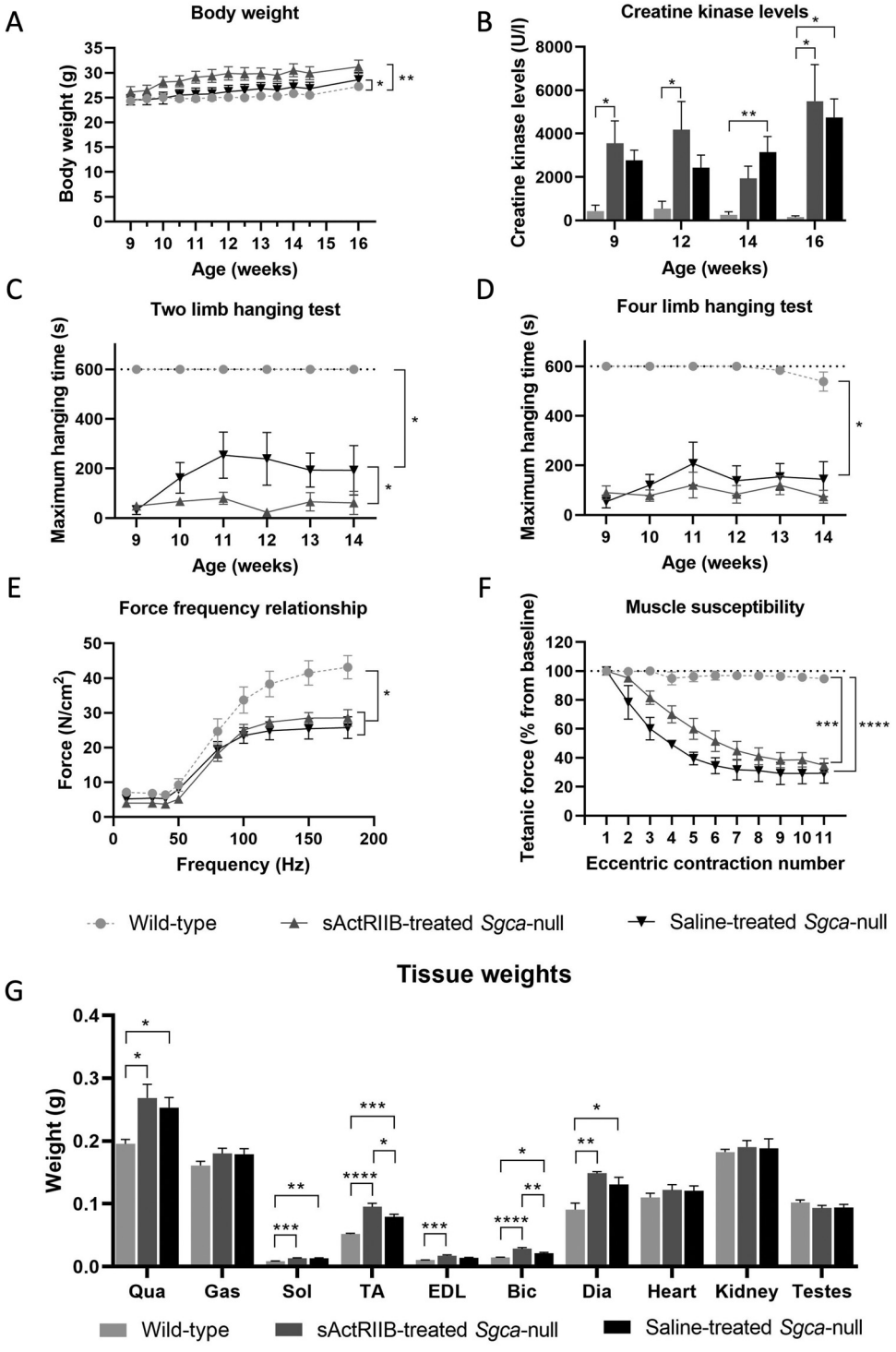

Fig. 5. Effect of sActRIIB-treatment on body weight, creatine kinase levels and muscle function when initiated at 9 weeks of age. (A) Bodyweight. (B) Creatine kinase levels. (C) Two limb hanging test. (D) Four limb hanging test. (E) Force frequency relationship in the tibialis anterior. (F) Susceptibility of the tibialis anterior to damage during eccentric contractions. (G) Tissue weights. $N=6$ per group. $^{*}P<0.05$, $^{**}P<0.01$, $^{***}P<0.001$, $^{****}P<0.0001$.

combination with a larger cross-sectional area for these IIA fibres in the soleus (Fig. 6D-E). Saline-treated *Sgca*-null mice had a statistically significant increase in proportion of IIX fibres in the soleus, compared to wild-type mice (Fig. 6D). For the tibialis anterior, we distinguish between the superficial (primarily fast-twitch) and deep (primarily slow-twitch) areas (Supplementary Fig. 6A). Here, we found no statistically significant difference between groups for the different fibre types in the superficial area of the tibialis anterior while type IIB fibres were statistically significantly decreased in the deep area of *Sgca*-null mice compared to wild-type (Supplementary Fig. 6B-C). We observed a

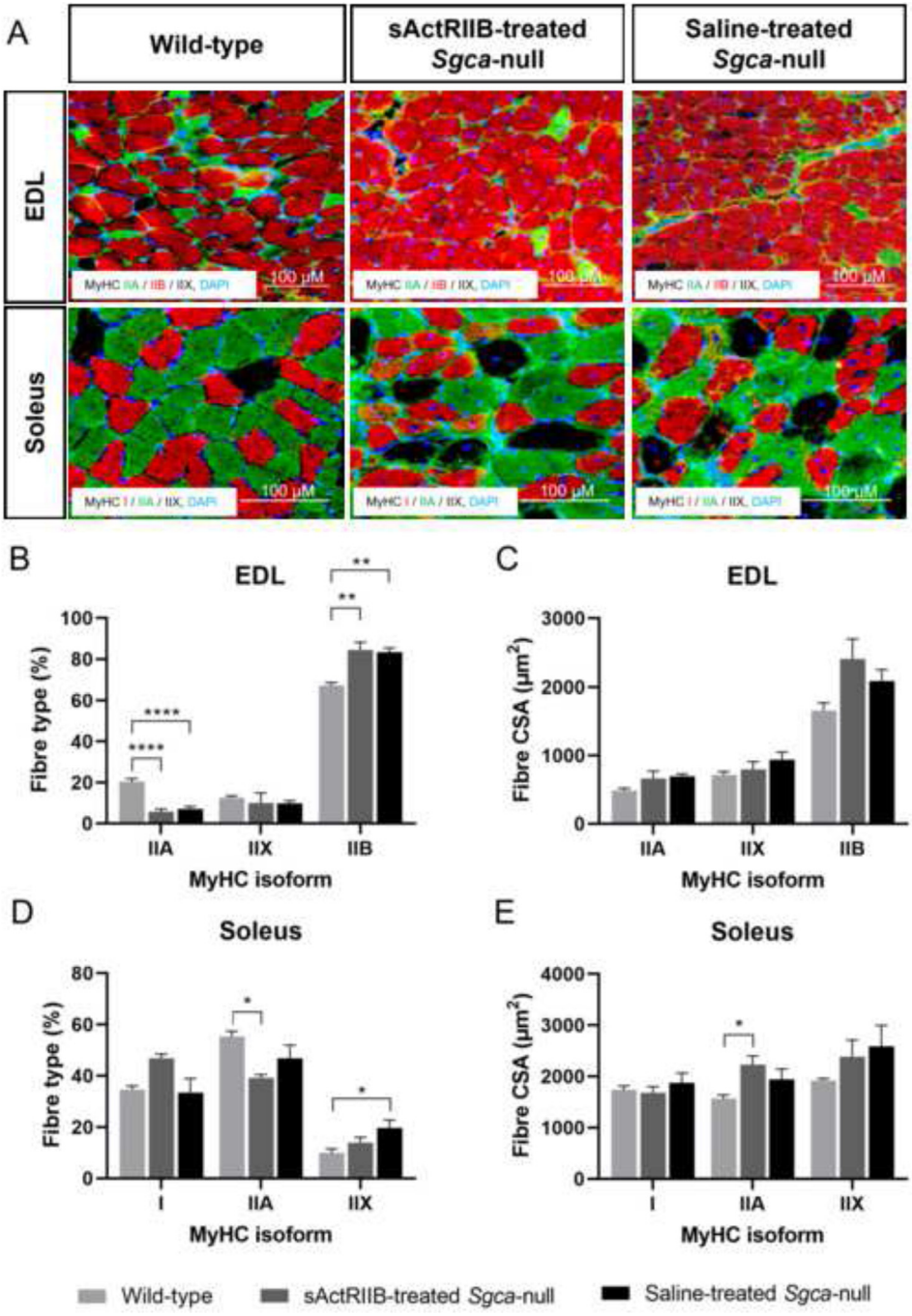

Fig. 6. Muscle fibre type changes after sActRIIB-treatment initiated at 9 weeks of age (A). Representative images of EDL, and soleus muscles from wild-type, sActRIIB-treated mice, and saline-treated mice; EDL: green= MyHC IIA, red= MyHC IIB, blue/DAPI = nuclei, soleus: green= MyHC IIA, red= MyHC Type I, blue/DAPI = nuclei. (B) MyHC fibre types IIA, IIX, and IIB percentage in EDL. (C) Fibre CSA of non-centrally nucleated MyHC isoforms in EDL. (D) MyHC fibre type I, IIA, and IIX percentage in soleus. (E) Fibre CSA of non-centrally nucleated MyHC isoform in soleus. $N=5$ per group $^{*}P<0.05$, $^{**}P<0.01$, $^{****}P<0.0001$.

shift towards smaller fibre cross-sectional areas for the different fibre types for *Sgca*-null, compared to wild-types, in both deep and superficial areas of the tibialis anterior (Supplementary Fig. 7).

As the cross-sectional area analysis of normal fibre types failed to offer an explanation for the increase in muscle mass induced by sActRIIB treatment, we examined the regenerating fibres. Profiling of the tibialis anterior, EDL and soleus revealed that the vast majority of fibres in both *Sgca*-null saline- and sActRIIB-treated groups had a centrally-located nucleus (Fig. 7A-B). Furthermore, the proportion of fibres with a centrally-located nuclei increased in all three muscles

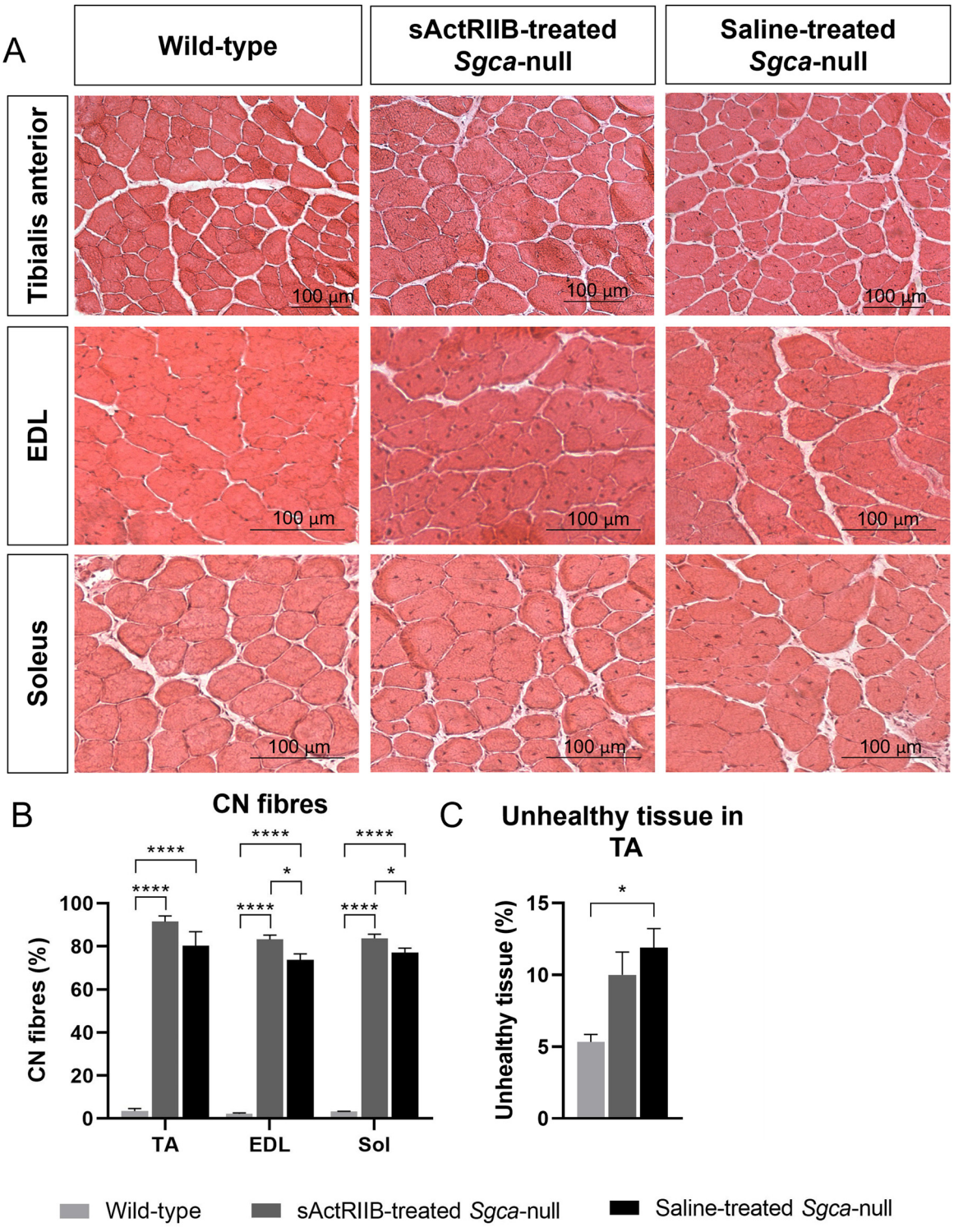

Fig. 7. Muscle histopathology of sActRIIB-treatment in mice being initiated at 9 weeks of age. (A) Representative images of H&E stained cross-sections of tibialis anterior (TA), EDL and soleus. (B) Quantification of the percentage of CN fibres in muscle sections. (C) Quantification of the percentage of unhealthy tissue in TA muscle; $N=5$ per group for EDL and soleus (Sol), $N=3$ per group for tibialis anterior. $^{*}P<0.05$, $^{****}P<0.0001$.

(reaching statistical significance in the EDL and soleus) in the sActRIIB-treated, compared to the saline-treated cohort (Fig. 7B). Examination of the non-muscle components revealed that the degree of fibrosis was unaffected by genotype or treatment (Supplementary Fig. 8A-B). Interestingly, the quantity of unhealthy tissue was only significantly increased in the saline-treated group when compared to wild-type (Fig. 7A,C). Quantification of sarcolemmal dystrophin expression revealed a genotype and treatment-based reduction in this parameter (Supplementary Fig. 8A,C). Analysis of the SDH profile

failed to reveal any impact of either genotype or treatment in either the EDL or soleus (Supplementary Fig. 9A-C).

3.6. sActRIIB treatment does not alter expression levels of regeneration, inflammation and adipogenesis markers in Sgca-null mice

The regeneration markers *Myh3, MyoG* and *Nox2* were statistically significantly increased in the gastrocnemius of *Sgca*-null mice, compared to wild-types, with an even further increase in *MyoG* expression observed in saline-treated *Sgca*-null mice compared to sActRIIB-treated *Sgca*-null mice (Fig. 8A, C-D). In the tibialis anterior, saline-treated *Sgca*-null mice had increased levels of *Myh3, Pax7, MyoG* and *Nox2* compared to wild-types and increased levels of *Nox2* compared to sActRIIB-treated mice (Fig. 8A-C). In the EDL, saline-treated *Sgca*-null mice had elevated levels of *MyoG* and *Nox2* compared to sActRIIB-treated *Sgca*-null and wild-type mice (Fig 8C-D).

Inflammation markers *Cd68* and *Lgals3* were statistically significantly increased in the tibialis anterior and EDL of saline-treated *Sgca*-null mice compared to both wild-types and sActRIIB-treated *Sgca*-null mice. Both *Sgca*-null groups had elevated levels of *Cd68* and *Lgals3* in the gastrocnemius compared to wild-types. *Lgals*3 was statistically significantly increased in the sActRIIB-treated *Sgca*-null mice compared to wild-types (Fig 8E-F).

The adipogenesis marker *Pparγ* was statistically significantly elevated in the tibialis anterior of saline-treated *Sgca*-null mice compared to wild-types. *Sgca*-null mice showed lower levels in the soleus but these were not statistically significant (Fig. 8G).

4. Discussion

Presently there are no treatments for limb girdle muscular dystrophy 2D (LGMD2D), although several interesting approaches are being evaluated not only in animal models but also, in a limited manner, in humans [18,19]. Whilst the conventional route for developing treatments for genetic disorders such as LGMD2D focus on replacing an aberrant gene, other therapeutic routes have been investigated especially for muscular disorders. One such alternate route to address the pathology is through promoting muscle growth using exogenous agents. Inhibition of myostatin, a negative regulator of muscle growth, is an interesting therapeutic target for the treatment of diseases that are characterized by muscle weakening and muscle loss [20,21]. Here, we studied the effects of myostatin inhibition with sActRIIB in *Sgca*-null mice in which treatment started either prior to the disease onset (week 3) or when mice were in the advanced stages of the disease (week 9).

4.1. Bodyweight changes and CK levels

Treatment with sActRIIB resulted in a pronounced increase in body and muscle weight in the *Sgca*-null mice regardless of the age of treatment initiation. This is in line with studies where *mdx* mice (model for Duchenne muscular dystrophy) were treated with 1 or 10 mg/kg sActRIIB twice weekly for 12 weeks starting at 4 weeks of age [11,12]. sActRIIB treatment in wild-type mice also resulted in significant increases in body weight and/or skeletal muscle mass [14,22,23]. While muscle mass increased upon sActRIIB treatment, plasma creatine kinase levels were similar in sActRIIB- and saline-treated *Sgca*-null mice. This might suggest that muscle membrane integrity improved when mice were treated with sActRIIB since one would otherwise expect higher CK levels because of the increase in diseased muscle mass. In contrast, treatment with sActRIIB in *mdx* mice resulted in decreased CK levels despite an increase in muscle mass. These contrasting results could be interpreted as the sActRIIB treatment being more effective in a less severely affected model (*mdx*) than the more severe model (*Sgca*) investigated here [12]..

4.2. Promotion of muscle growth

A previous study by Bartoli had the same aim but used AAV-mediated delivery of mutated myostatin propeptide in the same mouse model deployed in this study. Using the AAV viral delivery system they showed that the myostatin propeptide was able to promote robust muscle growth in a wild-type mouse. However, it had no effect on the LGMD2D model. Bartoli and colleagues demonstrated that the virus was unable to infect muscle cells and postulated that the inflammatory environment prevented this from taking place. However, recent work has shown that AAV viruses are more than capable of delivering gene cargoes to mouse LGMD2D muscle. The lack of infectivity described in the Bartoli work could be because of the use of a more inflammatory sensitive AAV virus (AAV-2/1) than that used by Griffin (AAVrh74, which is closely related to AAV-8) [24]. Not only is the mouse LGMD2D muscle prone to AAV infection (overturning the notion of Bartoli et al.) but is also able to undergo growth following the neutralisation of myostatin/activin. Nevertheless, the ability of sActRIIB to promote muscle growth was age-related. We found that administration of this molecule prior to the onset of muscle pathology provoked a much stronger hypertrophic response compared to when the intervention was applied when the disease was established. The decrease in potency of sActRIIB to promote muscle growth could be due to several factors, not least that the expression of the ligands that it binds may decrease as the pathology intensifies.

4.3. Muscle function

One of the main findings of this study was the negative correlation between sActRIIB-induced muscle growth and muscle function in the *Sgca*-null mice; muscle following sActRIIB-induced growth functioned worse compared to saline-treated *Sgca*-null mice, which might be partially due to the increased body weight. Moreover, when it failed to promote muscle growth, sActRIIB has no impact on muscle

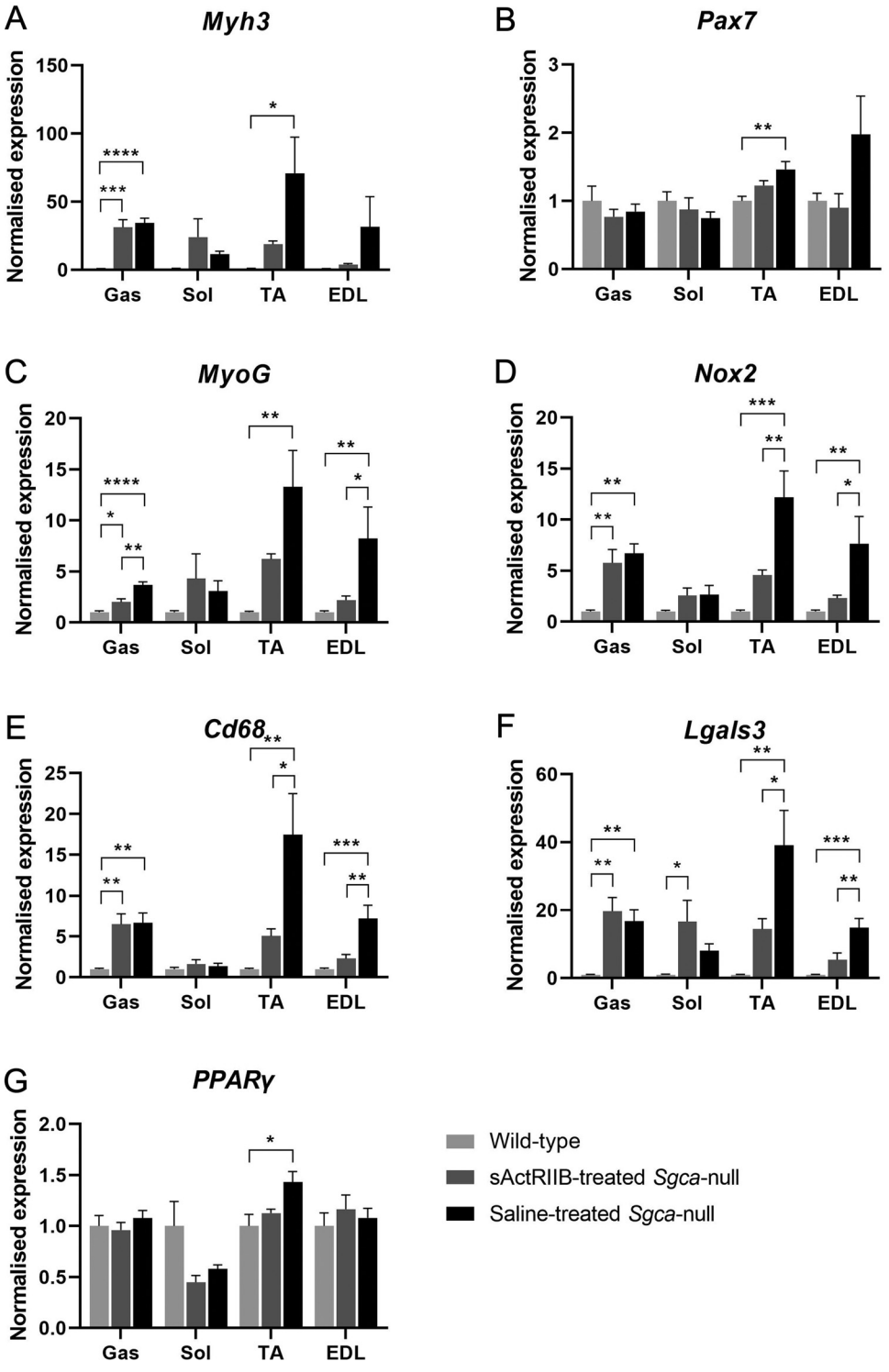

Fig. 8. Gene expression analyses of regeneration, inflammation and adipogenesis markers in mice in which sActRIIB treatment started at 9 weeks of age. (A-D) Regeneration markers *Myh3*, *Pax7, MyoG* and *Nox2,* (E-F) inflammation markers *Cd68* and *Lgals3* and (G) adipogenesis marker *Pparγ* in gastrocnemius (Gas), soleus (Sol), tibialis anterior (TA) and EDL. Expression levels were normalized for the housekeeping genes *Hmbs* (TA and Sol), *Hprt* (Gas) and *Gapdh* (EDL). $N=6$ per group. $^{*}P<0.05$, ** $P<0.01$, $^{***}P<0.001$, $^{****}P<0.0001$.

function deficit. Therefore, in the context of LGMD2D, when neutralisation of myostatin/activin results in muscle hypertrophy it leads to the development of a tissue that is physiologically compromised. This finding concords with a volume of evidence showing the same effect. Indeed, we conducted one of the first studies demonstrating that genetic deletion of myostatin leads to enlarged muscle with abnormally low specific force [9]. Additionally, we and

others have demonstrated that forced muscle growth in the *mdx* mouse model for DMD displayed profound fatigue characteristics [7,14]. We are currently investigating the reason why the treatment of *Sgca*-null mice with sActRIIB promotes muscle performance failure. Our study offers two explanations.

The first is based on the enlargement of muscle fibres. We suggest that muscle fibre hypertrophy in the absence of nuclear accretion leads to an increase in the myonuclear domain (MND), which is defined as the volume of cytoplasm serviced by each nuclei. It has been demonstrated that optimal muscle function is possible within a tightly defined MND and that either increasing or decreasing this parameter detrimentally impacts on force-generating capacity [25,26]. We show that muscle fibres, during the early stages of disease development, were larger than their wild-type counterpart and that the muscle showed partial functional impairment. However, when young *Sgca*-null mice were stimulated to undergo muscle fibre hypertrophy, it resulted in a tissue with significantly worse function. We suggest that expansion of the MND leads to a volume of cytoplasm containing organelles that cannot be properly serviced by the local nuclei.

The second explanation for the muscle phenotype could be based on the abnormally large muscle fibres that display a centrally located nuclei. The positioning of nuclei in muscle fibres is a highly regulated and dynamic process [27]. During muscle development, nuclei are located in the centre of immature fibres which thereafter translocate to the periphery [27]. Muscle regeneration, which recapitulates muscle development, also shows the displacement of nuclei to central positions within fibres and their subsequent movement to the periphery following fibre maturation (at least in humans). Centrally located nuclei are a hallmark of many neuromuscular disorders, including DMD [28]**.** There has been much speculation on the relationship between nuclei position and force generation. At the most simplistic level, it was assumed that a centrally located nucleus would interfere with the contractile apparatus. However, this seems to be unfounded. It was recently demonstrated that isolated single fibres harbouring centrally located nuclei perform just as well as those containing peripherally located nuclei [29]. However, this was only the case in normal muscle and not in genetic mutants where they showed that abnormal nuclear positioning was associated with a host of molecular abnormalities including suppressed transcriptional activity [29]. We note that the proportion of fibres harbouring centrally located nuclei were increased by sActRIIB treatment of *Sgca*-null mice, which correlated with a worsening of muscle function. The case for centrally located nuclei as a driver for attenuated muscle performance in *Sgca*-null mice is supported by a study showing that AAV-mediated delivery of alpha sarcoglycan reduced the proportion of fibres with centrally located nuclei, which was accompanied by improved muscle performance [24]. Collectively, these data suggest that centrally located nuclei are functionally tolerated by a normal genome, but that mutations to specific genes may initiate abnormal nuclear activities that compromise force generation when nuclei are centrally localized.

4.4. Conclusion

Inhibition of myostatin does not seem to have a positive effect on muscle function and pathology in *Sgca*-null mice. Since the defect of the dystrophin-glycoprotein complex is not resolved, more muscle does not equal better muscle and will only make the pathology worse when treatment with sActRIIB is started before disease onset. Possibly, a combination of myostatin inhibition with a therapy to target the primary defect could have a positive effect on disease pathology. This has been previously demonstrated in the *mdx* mouse model where combination therapy of dystrophin restoring therapy and sActRIIB, which either resulted in a similar effect in specific maximal force and resistance to eccentric contractions-induced damage in the tibialis anterior [30]. Controversially, other studies were not able to reproduce the synergic benefits of increasing specific maximal force in the TA muscle and increasing the muscle mass in combination therapy [7].

AAV delivery of α-sarcoglycan in $Sgca^{-/-}$ mice starting at 4 weeks of age resulted in expression in multiple muscles, including the diaphragm. Furthermore, this resulted in histopathology and specific force improvements in the tibialis anterior and diaphragm. Systemic gene transfer was deemed safe and effective [31].

Combinational therapies may have benefits in a disease-specific context. But there are still major questions whether it will be beneficial for LGDM2D. We demonstrated that attenuating myostatin/activin signalling compromised muscle function when it induced hypertrophy. In summary, our work suggests that attenuating myostatin/activin treatment does not inhibit disease progression of LGDM2D and even might exacerbate the disease.

Contributors

AA has contributed to the investigation, methodology, data curation, formal analysis and writing of the original draft. SE contributed to the investigation, methodology, data curation and formal analysis. AP and FC contributed to the investigation while CTdW and JP contributed with resources as well as the investigation. SV and AA-R were both involved in the study conceptualization and formal analysis. Furthermore, KP's contribution was in the study conceptualization, formal analysis, funding acquisition, administration, supervision, validation and writing of the original draft. MvP contributed to the conceptualization of the study, formal analysis funding acquisition and supervision. All authors contributed to reviewing and editing the manuscript.

Declaration of Competing Interest

The authors declare no competing interests.

Acknowledgements

This study was supported by the Prinses Beatrix Spierfonds (grant number W.OR1801) the Netherlands, Stichting Spieren voor Spieren the Netherlands, and by a PhD studentship funded by the Ministry of Defence in Kuwait. The experimental assistance provided by Kayleigh Putker was greatly appreciated.

Supplementary materials

Supplementary material associated with this article can be found, in the online version, at doi:10.1016/j.nmd.2022.03.002.

References

[1] Murphy AP, Straub V. The classification, natural history and treatment of the limb girdle muscular dystrophies. J Neuromuscul Dis 2015;2:S7–S19.
[2] Nigro V, Savarese M. Genetic basis of limb-girdle muscular dystrophies: the 2014 update. Acta Myol 2014;33:1–12.
[3] Cohn RD, Campbell KP. Molecular basis of muscular dystrophies. Muscle Nerve 2000;23:1456–71.
[4] Chu ML, Moran E. The limb-girdle muscular dystrophies: is treatment on the horizon? Neurotherapeutics 2018;15:849–862.
[5] Lee SJ, Reed LA, Davies MV, Girgenrath S, Goad ME, Tomkinson KN, et al. Regulation of muscle growth by multiple ligands signaling through activin type II receptors. Proc Natl Acad Sci U S A 2005;102:18117–22.
[6] Attie KM, Borgstein NG, Yang Y, Condon CH, Wilson DM, Pearsall AE, et al. A single ascending-dose study of muscle regulator ACE-031 in healthy volunteers. Muscle Nerve 2013;47:416–23.
[7] Hoogaars WM, Mouisel E, Pasternack A, Hulmi JJ, Relizani K, Schuelke M, et al. Combined effect of AAV-U7-induced dystrophin exon skipping and soluble activin Type IIB receptor in mdx mice. Hum Gene Ther 2012;23:1269–79.
[8] Elashry MI, Otto A, Matsakas A, El-Morsy SE, Patel K. Morphology and myofiber composition of skeletal musculature of the forelimb in young and aged wild type and myostatin null mice. Rejuvenation Res 2009;12:269–81.
[9] Amthor H, Macharia R, Navarrete R, Schuelke M, Brown SC, Otto A, et al. Lack of myostatin results in excessive muscle growth but impaired force generation. Proc Natl Acad Sci U S A 2007;104:1835–40.
[10] Amthor H, Hoogaars WM. Interference with myostatin/ActRIIB signaling as a therapeutic strategy for Duchenne muscular dystrophy. Curr Gene Ther 2012;12:245–59.
[11] Carlson CG, Bruemmer K, Sesti J, Stefanski C, Curtis H, Ucran J, et al. Soluble activin receptor type IIB increases forward pulling tension in the mdx mouse. Muscle Nerve 2011;43:694–9.
[12] Pistilli EE, Bogdanovich S, Goncalves MD, Ahima RS, Lachey J, Seehra J, et al. Targeting the activin type IIB receptor to improve muscle mass and function in the mdx mouse model of Duchenne muscular dystrophy. Am J Pathol 2011;178:1287–97.
[13] Campbell C, McMillan HJ, Mah JK, Tarnopolsky M, Selby K, McClure T, et al. Myostatin inhibitor ACE-031 treatment of ambulatory boys with Duchenne muscular dystrophy: results of a randomized, placebo-controlled clinical trial. Muscle Nerve 2017;55:458–64.
[14] Relizani K, Mouisel E, Giannesini B, Hourdé C, Patel K, Morales Gonzalez S, et al. Blockade of ActRIIB signaling triggers muscle fatigability and metabolic myopathy. Molecular Therapy: the journal of the American Society of Gene Therapy 2014;22:1423–33.
[15] Pasteuning-Vuhman S, Putker K, Tanganyika-de Winter CL, Boertje-van der Meulen JW, van Vliet L, Overzier M, et al. Natural disease history of mouse models for limb girdle muscular dystrophy types 2D and 2F. PLoS ONE 2017;12:e0182704.
[16] Verhaart IEC, Putker K, van de Vijver D, Tanganyika-de Winter CL, Pasteuning-Vuhman S, Plomp JJ, et al. Cross-sectional study into age-related pathology of mouse models for limb girdle muscular dystrophy types 2D and 2F. PLoS ONE 2019;14:e0220665.
[17] Aartsma-Rus A, van Putten M. Assessing functional performance in the mdx mouse model. Journal of visualized experiments: JoVE 2014.
[18] Mendell JR, Chicoine LG, Al-Zaidy SA, Sahenk Z, Lehman K, Lowes L, et al. Gene delivery for limb-girdle muscular dystrophy type 2D by isolated limb infusion. Hum Gene Ther 2019;30:794–801.
[19] Guha TK, Pichavant C, Calos MP. Plasmid-mediated gene therapy in mouse models of limb girdle muscular dystrophy. Mol Ther Methods Clin Dev 2019;15:294–304.
[20] Bartoli M, Poupiot J, Vulin A, Fougerousse F, Arandel L, Daniele N, et al. AAV-mediated delivery of a mutated myostatin propeptide ameliorates calpain 3 but not alpha-sarcoglycan deficiency. Gene Ther 2007;14:733–40.
[21] Nielsen TL, Vissing J, Krag TO. Antimyostatin treatment in health and disease: the story of great expectations and limited success. Cells 2021:10.
[22] Rahimov F, King OD, Warsing LC, Powell RE, Emerson CP Jr, Kunkel LM, et al. Gene expression profiling of skeletal muscles treated with a soluble activin type IIB receptor. Physiol Genomics 2011;43:398–407.
[23] Cadena SM, Tomkinson KN, Monnell TE, Spaits MS, Kumar R, Underwood KW, et al. Administration of a soluble activin type IIB receptor promotes skeletal muscle growth independent of fiber type. J Appl Physiol (1985) 2010;109:635–42.
[24] Griffin DA, Pozsgai ER, Heller KN, Potter RA, Peterson EL, Rodino-Klapac LR. Preclinical systemic delivery of adeno-associated α-sarcoglycan gene transfer for limb-girdle muscular dystrophy. Hum Gene Ther 2021;32:390–404.
[25] Omairi S, Matsakas A, Degens H, Kretz O, Hansson KA, Solbrå AV, et al. Enhanced exercise and regenerative capacity in a mouse model that violates size constraints of oxidative muscle fibres. Elife 2016;5.
[26] Otto A, Macharia R, Matsakas A, Valasek P, Mankoo BS, Patel K. A hypoplastic model of skeletal muscle development displaying reduced foetal myoblast cell numbers, increased oxidative myofibres and improved specific tension capacity. Dev. Biol. 2010;343:51–62.
[27] Roman W, Gomes ER. Nuclear positioning in skeletal muscle. Semin. Cell Dev. Biol. 2018;82:51–6.
[28] Sjöberg G, Edström L, Lendahl U, Sejersen T. Myofibers from Duchenne/Becker muscular dystrophy and myositis express the intermediate filament nestin. J Neuropathol Exp Neurol 1994;53:416–23.
[29] Ross JA, Tasfaout H, Levy Y, Morgan J, Cowling BS, Laporte J, et al. rAAV-related therapy fully rescues myonuclear and myofilament function in X-linked myotubular myopathy. Acta Neuropathol Commun 2020;8:167.
[30] Dumonceaux J, Marie S, Beley C, Trollet C, Vignaud A, Ferry A, et al. Combination of myostatin pathway interference and dystrophin rescue enhances tetanic and specific force in dystrophic mdx mice. Molecular Therapy: the journal of the American Society of Gene Therapy 2010;18:881–7.
[31] Griffin DA, Pozsgai ER, Heller KN, Potter RA, Peterson EL, Rodino-Klapac LR. Preclinical systemic delivery of adeno-associated alpha-sarcoglycan gene transfer for limb-girdle muscular dystrophy. Hum Gene Ther 2021.